States near Dirac points of a rectangular graphene dot in a magnetic field

S. C. Kim,[1] P. S. Park,[1] and S.-R. Eric Yang[1,2,*]
[1]*Physics Department, Korea University, Seoul, Korea*
[2]*Korea Institute for Advanced Study, Seoul, Korea*

(Received 15 June 2009; revised manuscript received 28 December 2009; published 23 February 2010)

In neutral graphene dots, the Fermi level coincides with the Dirac points. We have investigated in the presence of a magnetic field several unusual properties of single electron states near the Fermi level of such a rectangular-shaped graphene dot with two zigzag and two armchair edges. We find that a quasidegenerate level forms near zero energy and the number of states in this level can be tuned by the magnetic field. The wave functions of states in this level are all peaked on the zigzag edges with or without some weight inside the dot. Some of these states are magnetic field-independent surface states while the others are field-dependent. We have found a scaling result from which the number of magnetic field-dependent states of large dots can be inferred from those of smaller dots.

DOI: 10.1103/PhysRevB.81.085432 PACS number(s): 73.20.At, 73.22.−f, 81.05.U−

I. INTRODUCTION

Graphene dots have a great potential for many applications since they are the elemental blocks to construct graphene-based nanodevices. It is possible to cut graphene sheet[1] in the desired shape and size[2] and use it to make quantum dot devices. In such devices, it may be possible to realize experimentally zigzag or armchair boundaries.

Graphene systems possess several unusual physical properties associated with the presence of the Dirac points. For example, compared to ordinary Landau levels of quasi-two-dimensional semiconductors the lowest Landau level (LLL) of graphene is peculiar since it has *zero* energy that is independent of magnetic field.[3–7] Moreover, wave functions of the LLL are *chiral*, i.e., the probability amplitude of find the electron on one type carbon atoms is zero. There are other graphene systems with zero energy states. Semi-infinite[8] or nanoribbon graphene[9,10] with zigzag edges along the x axis develop a flat band of *zero* energy chiral states. These states are surface states and are localized states at the zigzag edges with various localization lengths.[8] The zigzag edge and the LLL states have zero energy because their wave functions are chiral. Effects of a magnetic field on graphene Hall bars have been investigated recently, and some zero energy chiral states are found to be strongly localized on the zigzag edges in addition to the usual LLL states.[11–14]

One may expect that the degeneracy of chiral states with zero energy will be split when quantum confinement effect is introduced in a graphene dot.[15–17] However, the splitting of these energies may be unusual in some graphene dots.[18–21] Recently, the magnetic field dependence of these levels in a gated graphene dot was investigated experimentally.[21] Effects of various types of edges have been also investigated: zigzag-edged dots, armchair-edged dots,[19,22–24] and rectangular graphene dots with two zigzag and two armchair edges[25,26] have been studied. Armchair edges couple states near K and K′ points of the first Brillouin zone and generate several mixed chiral zigzag edge states with *nearly* zero energies. In the rectangular dots the number of these states, N_l, may be determined from the condition that the x component of wavevectors satisfies $1/L_y < k_{x,n} < \pi/3a$, where $k_{x,n} = \frac{\pi n}{L_x} - \frac{2\pi}{3a}$, $a = \sqrt{3}a_0$ is the length of the unit cell, and $n = 0, \pm 1, \pm 2, \ldots$ (the nearest neighbor carbon-carbon distance is $a_0 = 1.42$ Å, the horizontal length of the dot is $L_x = \sqrt{3}Ma_0$ with M number of hexagons along the x axis, and the vertical length is $L_y = a_0(3N+2)$ with N the number of hexagons and $(N+1)$ carbon bonds along the y axis. See Fig. 1). This condition implies that the integer n is given by

$$\frac{\sqrt{3}M}{(3N+2)\pi} + \frac{2M}{3} \leq n \leq M. \tag{1}$$

The effective mass approximation wave functions of these surface states are derived in Ref. 26.

We investigate how properties of rectangular dots change in the presence of a magnetic field in the regime where Hofstadter butterfly effects[18,19,21] are negligible. In neutral graphene dots, the Fermi level has zero energy, and, consequently, magnetic, optical, and STM (scanning tunneling microscopy) properties are expected to depend on the number of available states near zero energy. Our investigation shows that the wave functions of nearly zero energy states are all peaked on the zigzag edges with or without appreciable weight inside the dot. This may be understood as mixing of LLL and surface states by armchair edges of the rectangular dot through intervalley scattering, which is unique to the rectangular dot (this will be explained in Sec. IV).

Our study shows that the number of states within the energy interval δ around zero energy is given by

$$N_T(\phi) = N_l + N_D(\phi) \tag{2}$$

(the energy δ is typically less than the quantization energy of a rectangular dot, which can be estimated using the Dirac equation: $\gamma k_{\min} \sim t\frac{a}{L_{x,y}}$, where $\gamma = \sqrt{3}ta/2$ with the hopping energy t). Here, magnetic edge states are not included since their energies are larger than δ. $N_D(\phi)$ is the number states that merge into the energy interval δ around zero energy as the dimensionless magnetic flux $\phi = \frac{\Phi}{\Phi_0}$ increases. This effect provides a means to control the number of states at the Fermi level. There are other states with nearly zero energies at $\phi = 0$, which remain so even at $\phi \neq 0$. The localization lengths

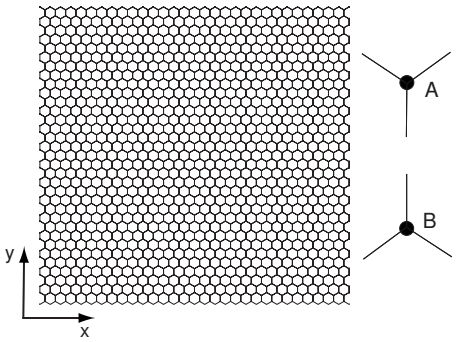

FIG. 1. Finite graphene layer with zigzag and armchair edges. There are equal number of A and B carbon atoms. The graphene layer has reflection symmetries about horizontal and vertical lines that go through the center of the layer. A magnetic field is present perpendicular to the layer.

of these states are shorter than the magnetic length. We denote the number of these states by N_l.

Our numerical results indicate that for relatively small rectangular-shaped graphene dots with size less than on order 10^2 Å, the number of states at the Fermi level display a negligible magnetic field dependence for values that are usually accessible experimentally ($B<10$ T corresponds, in dimensionless magnetic flux, to $\phi=\frac{\Phi}{\Phi_0}<10^{-4}$, where $\Phi_0=hc/e$ and $\Phi=BA_h$ with the area of a hexagon $A_h=\frac{3\sqrt{3}}{2}a_0^2$). On the other hand, in larger dots this dependence is significant. However, it is computationally difficult to investigate large rectangular-shaped graphene dots since the number of carbon atoms increases rapidly with the size. We have found a scaling result from which one can infer results for larger dots from those of smaller dots. For different rectangular-shaped graphene dots and values of ϕ, it can be described well by the following dimensionless form:

$$N_D(\phi)=\frac{L_xL_y}{A_h}f\left(\frac{\ell^2}{a_0(L_x+L_y)}\right), \tag{3}$$

where $\ell=\frac{3^{3/4}a_0}{(4\pi\phi)^{1/2}}$ is the magnetic length and $f(x)$ is a scaling function, see Fig. 2. The total number of hexagons in the dot is $N_h=L_xL_y/A_h$. Our numerical result shows that the dependence of $N_D(\phi)$ on ϕ is initially nonlinear in the regime where the diameter of the cyclotron motion is comparable to the system length, $2\ell\sim L_{x,y}$.

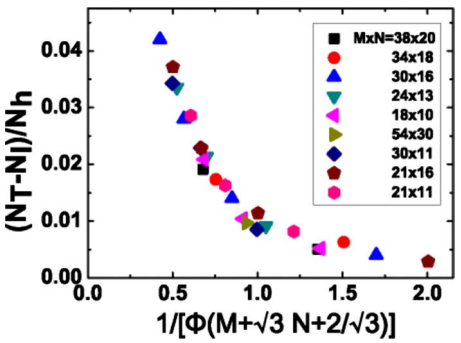

FIG. 2. (Color online) Number of nearly zero energy states that are induced by a magnetic field follow a scaling curve when plotted as a function of $\frac{1}{(M+\sqrt{3}N+2/\sqrt{3})\phi}$ for different rectangular shaped graphene dots. Here, $\delta=0.01$ eV.

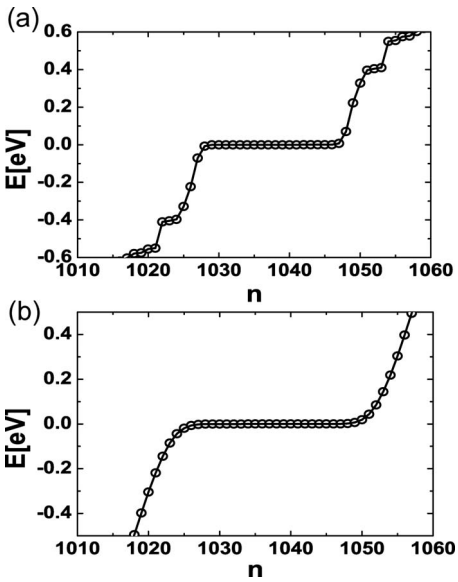

FIG. 3. (a) Eigenenergies ϵ_n at $\phi=0$. Quasidegenerate states are present near zero energy. Size of the dot is 74×71 Å^2. A quantization energy of order $\gamma k_{\min}\sim0.03$ eV can be seen as an excitation gap near zero energy. (b) Eigenenergies ϵ_n at $\phi=0.01$.

II. NUMBER OF STATES IN THE QUASIDEGENERATE LEVEL

Our Hamiltonian is

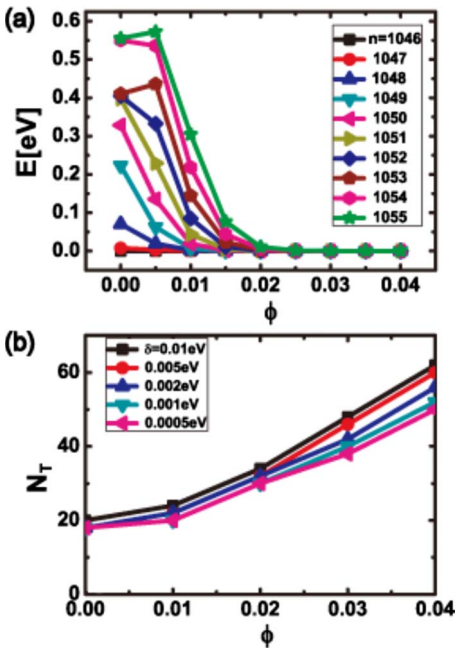

FIG. 4. (Color online) (a) Some energy levels ϵ_n change as ϕ increases while some do not. (b) The total number of states within the energy interval δ around zero energy at a finite value of ϕ. Size of the dot is 74×71 Å^2.

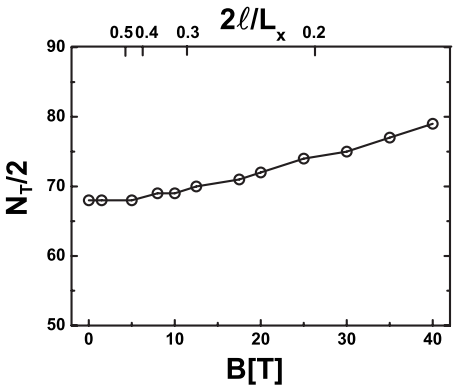

FIG. 5. Results for a dot with size 50×50 nm^2. Dependence of $N_T/2$ on B for $\delta=0.01$ eV.

$$H=-\sum_{\langle i,j\rangle} t_{ij}c_i^{\dagger}c_j, \tag{4}$$

where $t_{ij}=te^{i(e/\hbar)\int_{R_j}^{\vec{R}_i}\vec{A}\cdot d\vec{r}}$ are the hopping parameters and c_i^{+} creates an electron at site i. Here, we use a Landau gauge $\vec{A}=B(-y,0,0)$. The summation $\langle i,j\rangle$ is over nearest neighbor sites and $t=2.5$ eV. The eigenstate with eigenenergy ϵ_n is denoted by $\phi_{\epsilon_n}(\vec{R})$, where $\vec{R}$ labels each lattice point. Because of electron-hole symmetry, eigenvalues appear in pairs of positive and negative values $(\epsilon,-\epsilon)$, and the probability wave functions of a pair of states, $(|\phi_{\epsilon_n}(\vec{R})|^2,|\phi_{-\epsilon_n}(\vec{R})|^2)$, are identical. Our numerical results are consistent with this.

Figures 3(a) and 3(b) display the energy spectra near zero energy for $\phi=0$ and 0.01. At $\phi=0$, there are approximately 20 states within $|\epsilon_n|<0.01$ eV, consistent with the analytical result of Eq. (1). At $\phi=0.01$, the numerical value is increased to 24. Figure 4(a) shows how some energy levels ϵ_n at $\phi=0$ change as a function of the magnetic flux ϕ. These energy levels do not anticross. We observe that nearly zero energies at $\phi=0$ do not change noticeably in magnitude as ϕ varies. There are N_l such localized surface states. On the other hand, we find that as ϕ increases nonzero energies become smaller and move closer to zero. This implies that, for a given energy interval δ, the number of states in it, $N_T(\phi)$, increases with ϕ. From Fig. 4(b), we see that it displays a nonlinear dependence on ϕ. For a large dot of size 50×50 nm^2 a similar dependence of N_T on B is seen, as shown in Fig. 5. Nonlinear dependence occurs in the regime $2\ell/L_x\sim 0.5$. As a test of our numerical procedures we have verified that the sum of $N_D(\phi)=N_T(\phi)-N_l$ and the number of magnetic edge states is equal to the total bulk Landau level degeneracy $2D_B$ ($D_B=\frac{2L_xL_y}{3\sqrt{3}a_0^2}\phi$ is the degeneracy per valley).

The ratio between the number of nearly zero energy states induced by the magnetic field and the number of hexagons, $\frac{N_D(\phi)}{N_h}$, should depend on a dimensionless quantity consisting of a combination of ℓ, a_0, L_x, and L_y, which are the important parameters of rectangular graphene dots. The lengths L_x and L_y should appear as L_x+L_y so that for rectangular-shaped graphene sheets N_D/N_h remains the same when L_x and L_y are exchanged. These considerations lead us to the dimensionless variable $\frac{\ell^2}{a_0(L_x+L_y)}=\frac{3}{4\pi}\frac{1}{\phi(M+\sqrt{3}N+2/\sqrt{3})}$, see Eq. (3). We are especially interested in the regime where the diameter of the cyclotron orbit is comparable to the system length $2\ell\sim L_{x,y}$. Note that in this regime, many cyclotron orbits get affected by the presence of the edges and corners of the rectangular dot. Since we must also assume that Hofstadter effect is neg-

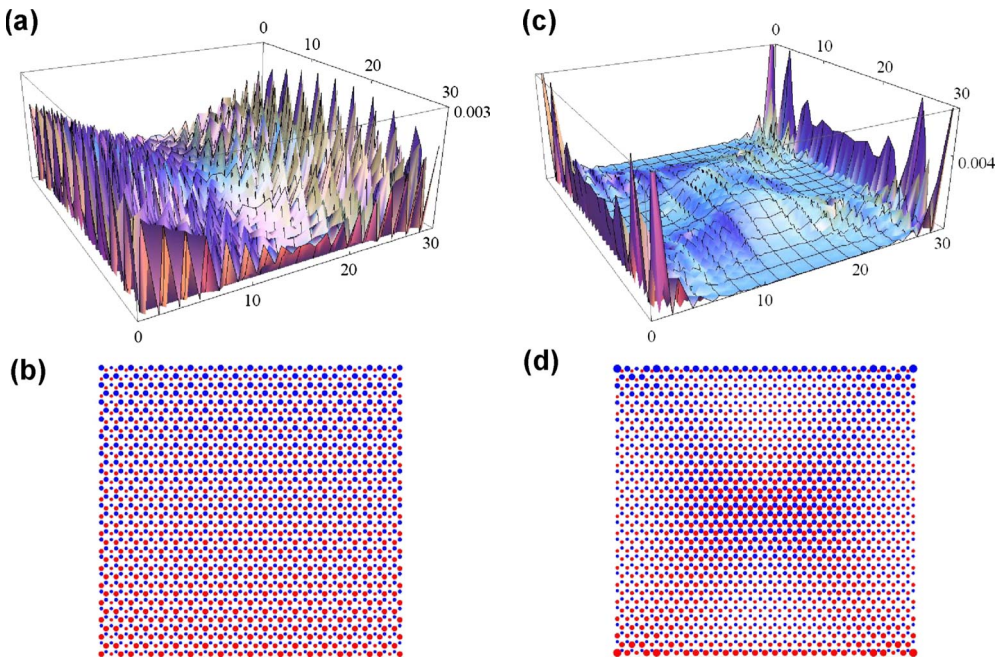

FIG. 6. (Color online) Size of the dot is 74×71 Å^2. (a) The probability wave function of the state with $\epsilon_{1027}=-0.07$ eV at $\phi=0$. The length unit is a. (b) Profile of z component of pseudospin: sizes of dots represent probabilities of occupying A or B carbon atoms. When the probabilities are less than 0.00001, the radius of the dots is set to the smallest value. The upper and lower horizontal edges represent zigzag edges. (c) The probability wave function of the state with $\epsilon_{1027}=-2.0\times 10^{-3}$ eV at $\ell/L_x=0.12$ ($\phi=0.01$). (d) Profile of z component of pseudospin for $n=1027$ at $\phi=0.01$.

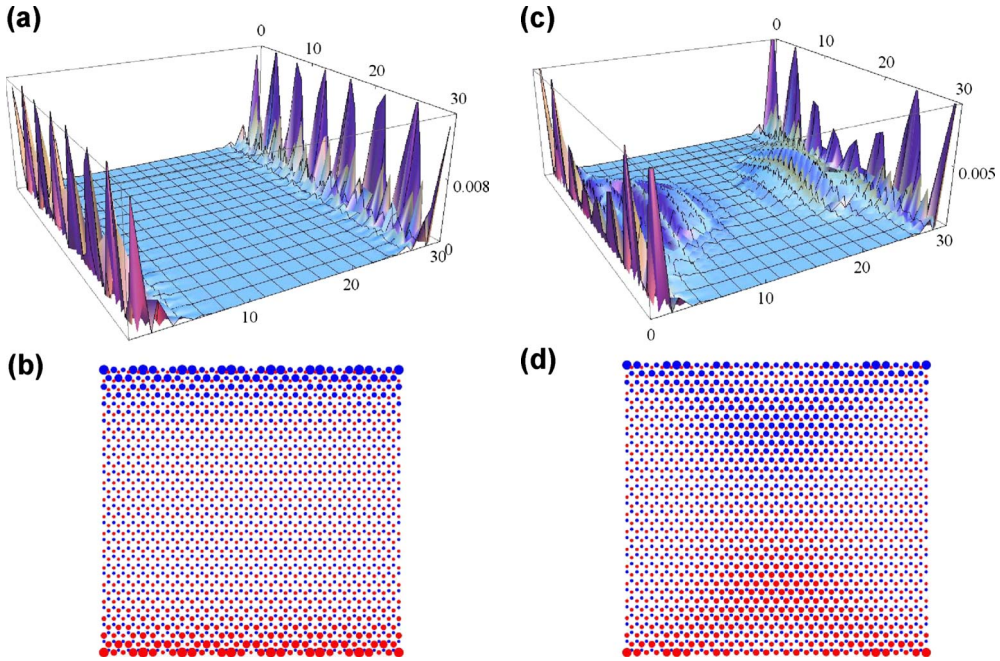

FIG. 7. (Color online) Size of the dot is 74×71 Å^2. (a) The probability wave function of the state with $\epsilon_{1045}=5.38\times10^{-6}$ eV at $\phi=0$. (b) Profile of z component of pseudospin for $n=1045$ at $\phi=0$. (c) The probability wave function for $n=1045$ at $\ell/L_x=0.12$ ($\phi=0.01$). (d) Profile of z component of pseudospin for $n=1045$ at $\phi=0.01$.

ligible the validity regime of Eq. (3) is $a_0 \ll 2\ell < L_{x,y}$. Note also that the scaling function $f(x)$ should be different for each δ.

III. WAVE FUNCTIONS OF QUASIDEGENERATE STATES IN A MAGNETIC FIELD

We first show how the wave function of a nonzero energy state at $\phi=0$ changes into a state with nearly zero energy as ϕ increases. Consider the probability wave function for $n=1027$ at a finite $\phi=0.01$, as shown in Fig. 6(c). It is localized on the zigzag edges with a finite probability inside the dot. On the armchair edges the wave function is vanishingly small. The wave function has changed significantly from the $\phi=0$ result, see Fig. 6(a), and also its energy has changed from -0.07 eV to -2.0×10^{-3} eV. The values of the z component of the pseudospin, Figs. 6(b) and 6(d), are larger on the zigzag edges at $\phi=0.01$ compared to the result at $\phi=0$. The probability wave function of another state with nearly zero energy is shown in Fig. 7(c) at $\phi=0.01$. We see that the result is somewhat different from the zero field result of Fig. 7(a), which displays a localized state with the localization length comparable to the unit cell length a. Now, there is a finite probability to find an electron inside the dot while the probabilities on the zigzag edges are reduced. Note that the energy of this state has changed from 5.38×10^{-6} eV to 4.5×10^{-6} eV when ϕ is changed to 0.01 from zero. The pseudospin profiles are shown in Figs. 7(b) and 7(d). Figure 8 shows a probability wave function at a smaller value of $\ell/L_{x,y}=0.09$ (corresponding to $\phi=0.02$), and we see that the wave function is less localized on the zigzag edges and LLL character is more pronounced in comparison to result of $\ell/L_x=0.12$ [Fig. 6(c)]. All $N_D(\phi)$ states have similar properties mentioned above with finite probabilities of finding an electron inside the dot. There are also N_ℓ zigzag edges states that are more strongly localized on the edges with localization lengths comparable to a. When an electron is in one of these states the probability of find the electron away from the edges is practically zero. The energies of these states are less then 10^{-10} eV. We can summarize our results as follows: all

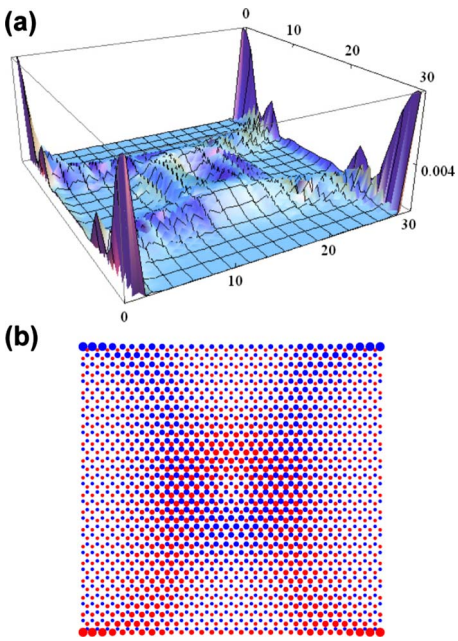

FIG. 8. (Color online) Size of the dot is 74×71 Å^2 and $\ell/L_x=0.09$ ($\phi=0.02$) (a) The probability wave function of the state with $\epsilon_{1027}=-2.04\times10^{-5}$ eV. (b) Profile of z component of pseudospin of the same state. These results should compare with those in Fig. 6.

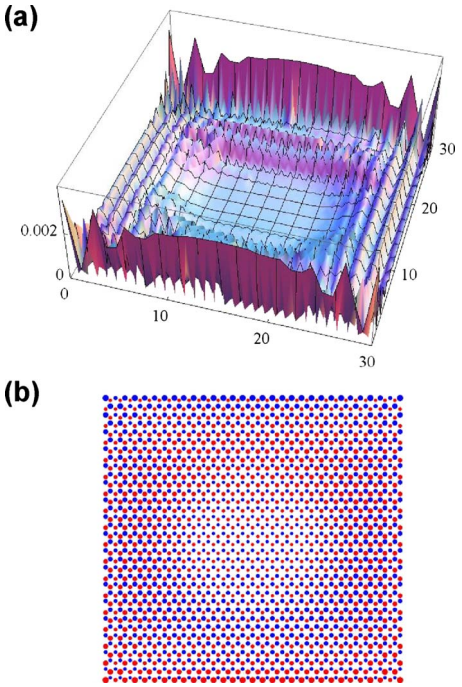

FIG. 9. (Color online) (a) The probability wave function of the state with $\epsilon_{1053}=0.144$ eV at $\ell/L_x=0.12$ ($\phi=0.01$). Size of the dot is 74×71 Å^2. (b) Profile of z component of pseudospin of the same state.

nearly zero energy states are localized on the zigzag edges with or without some weight inside the dot.

When the magnetic length is much smaller than the system size magnetic edge states can be formed, see Fig. 9. The probability wave function of a magnetic edge state with $\epsilon_{1053}=0.144$ eV is shown in Fig. 9(a). It is a mixture of ordinary magnetic and zigzag edge states. The probability wave function decays from the armchair edges while it is strongly peaked on the zigzag edges. Pseudospin expectation values on each zigzag edge display opposite chiral behavior. On armchair edges, the chiralities are more or less evenly mixed, see Fig. 9(b).

IV. DISCUSSIONS AND CONCLUSIONS

We now explain qualitatively how mixed states of Figs. 6(c) and 7(c) can arise. An infinitely long zigzag nanoribbon in a magnetic field has nearly zero energy surface states that are localized on the edges in addition to ordinary lowest Landau level states, see Fig. 10. The properties of these states are given in Refs. 6, 11, 12, 31, and 32: LLL states of valley K (K′) are of B (A) type and localized surface states have a mixed character between A and B. The surface states can have various localization lengths but the minimum value is of order the carbon-carbon distance a_0.[12] The armchair edges couple K and K′ valleys,[6,11,26] and, consequently, surface and LLL states of a nanoribbon can be coupled and give rise to mixed states with significant weight on the zigzag edges and inside the dot, as shown in Fig. 6(c) and Fig. 7(c). In addition, these mixed states should display a significant occupation of both A and B carbon atoms inside the dot since LLL states of different chiralities are coupled by the armchair edges. Our numerical result is indeed consistent with this expectation, see Fig. 6(d). As the ratio $\ell/L_{x,y}$ takes smaller values the nature of these states become more like that of LLL states (see Fig. 8).

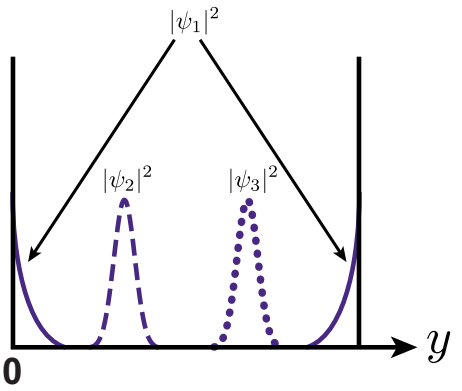

FIG. 10. (Color online) Cross section of probability wave functions of a nanoribbon with infinitely long zigzag edges along the x axis in the presence of a perpendicular magnetic field (a Landau gauge is used). $|\psi_1|^2$ represents a localized surface state. Two examples of LLL states $|\psi_2|^2$ and $|\psi_3|^2$ are also shown. These states all have nearly zero energies.

We have investigated, in the presence of a magnetic field, quasidegenerate states of rectangular-shaped graphene dots near the Dirac points. Some of these states are magnetic field-independent surface states while the other states are field-dependent. We find numerically that the wave functions of these states are all peaked near the zigzag edges with or without significant weight inside the dot. The physical origin of the presence of a significant weight is the coupling between K and K′ valleys due to the armchair edges. This effect is expected to survive small deviations from perfect armchair edges as long as they provide coupling between different valleys. Experimentally the dependence of N_D on ϕ may be studied by measuring STM properties[27] or the optical absorption spectrum as a function of magnetic field.[28–30] In fabricating rectangular dots, a special attention should be given to the direction of armchair edges since the properties of dot may depend on it.[33]

ACKNOWLEDGMENTS

This work was supported by the Korea Research Foundation Grant funded by the Korean Government (Grant No. KRF-2009-0074470). In addition, this work was supported by the Second Brain Korea 21 Project.

*Corresponding author; eyang@venus.korea.ac.kr

[1] For recent reviews, see T. Ando, J. Phys. Soc. Jpn. **74**, 777 (2005); A. K. Geim and A. H. MacDonald, Phys. Today **60**, 35 (2007); A. H. Castro Neto, F. Guinea, N. M. R. Peres, K. S. Novoselov, and A. K. Geim, Rev. Mod. Phys. **81**, 109 (2009).

[2] K. S. Novoselov, A. K. Geim, S. V. Morozov, D. Jiang, Y. Zhang, S. V. Dubonos, I. V. Grigorieva, and A. A. Firsov, Science **306**, 666 (2004); H. Hiura, Appl. Surf. Sci. **222**, 374 (2004); A. K. Geim and K. S. Novoselov, Nature Mater. **6**, 183 (2007).

[3] Y. Zhang, Y. W. Tan, H. L. Stormer, and P. Kim, Nature (London) **438**, 201 (2005).

[4] K. S. Novoselov, A. K. Geim, S. V. Morozov, D. Jiang, M. I. Katsnelson, I. V. Grigorieva, S. V. Dubonos, and A. A. Firsov, Nature (London) **438**, 197 (2005).

[5] J. W. McClure, Phys. Rev. **104**, 666 (1956).

[6] Y. Zheng and T. Ando, Phys. Rev. B **65**, 245420 (2002).

[7] S. G. Sharapov, V. P. Gusynin, and H. Beck, Phys. Rev. B **69**, 075104 (2004).

[8] M. Fujita, K. Wakabayashi, K. Nakada, and K. Kusakabe, J. Phys. Soc. Jpn. **65**, 1920 (1996).

[9] L. Brey and H. A. Fertig, Phys. Rev. B **73**, 195408 (2006).

[10] Y. W. Son, M. L. Cohen, and S. G. Louie, Phys. Rev. Lett. **97**, 216803 (2006).

[11] L. Brey and H. A. Fertig, Phys. Rev. B **73**, 235411 (2006).

[12] A. H. Castro Neto, F. Guinea, and N. M. R. Peres, Phys. Rev. B **73**, 205408 (2006).

[13] V. P. Gusynin, V. A. Miransky, S. G. Sharapov, I. A. Shovkovy, and C. M. Wyenberg, Phys. Rev. B **79**, 115431 (2009).

[14] M. Arikawa, Y. Hatsugai, and H. Aoki, Phys. Rev. B **78**, 205401 (2008).

[15] A. DeMartino, L. Dell'Anna, and R. Egger, Phys. Rev. Lett. **98**, 066802 (2007).

[16] G. Giavaras, P. A. Maksym, and M. Roy, J. Phys.: Condens. Matter **21**, 102201 (2009).

[17] W. Häusler and R. Egger, Phys. Rev. B **80**, 161402(R) (2009).

[18] S. Schnez, K. Ensslin, M. Sigrist, and T. Ihn, Phys. Rev. B **78**, 195427 (2008).

[19] Z. Z. Zhang, K. Chang, and F. M. Peeters, Phys. Rev. B **77**, 235411 (2008).

[20] P. Recher, J. Nilsson, G. Burkard, and B. Trauzettel, Phys. Rev. B **79**, 085407 (2009).

[21] J. Güttinger, C. Stampfer, F. Libisch, T. Frey, J. Burgdörfer, T. Ihn, and K. Ensslin, Phys. Rev. Lett. **103**, 046810 (2009).

[22] J. Fernández-Rossier and J. J. Palacios, Phys. Rev. Lett. **99**, 177204 (2007).

[23] M. Ezawa, Phys. Rev. B **76**, 245415 (2007).

[24] O. Hod, V. Barone, and G. E. Scuseria, Phys. Rev. B **77**, 035411 (2008).

[25] B. Trauzettel, D. V. Bulaev, D. Loss, and G. Burkard, Nat. Phys. **3**, 192 (2007).

[26] C. Tang, W. Yan, Y. Zheng, G. Li, and L. Li, Nanotechnology **19**, 435401 (2008).

[27] Y. Niimi, H. Kambara, T. Matsui, D. Yoshioka, and H. Fukuyama, Phys. Rev. Lett. **97**, 236804 (2006).

[28] M. O. Goerbig, J.-N. Fuchs, K. Kechedzhi, and V. I. Fal'ko, Phys. Rev. Lett. **99**, 087402 (2007).

[29] V. P. Gusynin, S. G. Sharapov, and J. P. Carbotte, Phys. Rev. Lett. **98**, 157402 (2007).

[30] H. Hsu and L. E. Reichl, Phys. Rev. B **76**, 045418 (2007).

[31] M. Kohmoto and Y. Hasegawa, Phys. Rev. B **76**, 205402 (2007).

[32] L. Brey and H. A. Fertig, Phys. Rev. B **75**, 125434 (2007).

[33] A. R. Akhmerov and C. W. J. Beenakker, Phys. Rev. B **77**, 085423 (2008).